



Received: 2016.09.18
Accepted: 2016.10.11
Published: 2017.06.25

Authors' Contribution:

- A** Study Design
- B** Data Collection
- C** Statistical Analysis
- D** Data Interpretation
- E** Manuscript Preparation
- F** Literature Search
- G** Funds Collection

Utility of Plain Radiographs in Metabolic Bone Disease – A Case-Based Pictorial Review from a Tertiary Centre

Jyoti Panwar^{1,2}**ABCDEF**, Ashish Jacob Mathew³**EF**, Nancy Jindal¹**G**, Debashish Danda³**E**

¹ Department of Radiology, Christian Medical College, Vellore, Tamilnadu, India

² Joint Department of Medical Imaging, University of Toronto, Toronto, ON, Canada

³ Department of Clinical Immunology and Rheumatology, Christian Medical College, Vellore, Tamilnadu, India

Author's address: Jyoti Panwar, Joint Department of Medical Imaging, University of Toronto, Toronto General Hospital, Munk Building, 1 PMB-298, 585 University Avenue, Toronto, Ontario, M5G 2N2, Canada, e-mail: drjyotimch@gmail.com

Summary

In this era of advanced high-tech imaging, the utility of plain radiographs in conditions of the bone is increasingly being overseen by both clinicians and radiologists. Plain radiography is the first-line, essential screening or diagnostic tool for diverse bone diseases, where magnetic resonance imaging (MRI) may be non-contributory. Plain radiographs often play a pivotal role in diagnosing metabolic bone disorders. This paper from a single tertiary care centre discusses ten real-life patients with metabolic bone conditions and other bone diseases with near-normal MRI of the spine, in whom plain radiographs revealed subtle findings and aided in making diagnoses.

Each of these cases had a non-specific clinical presentation. They all showed inconclusive features on MRI, but subtle important radiographic findings led to a specific diagnosis.

Plain radiography is key in diagnosing bone diseases. Many of these metabolic conditions clinically mimic rheumatologic conditions owing to non-specific arthralgia and back pain. Familiarity with subtle radiographic findings of these conditions may lead to early diagnosis and treatment, resulting in improved patient outcomes.

MeSH Keywords: Bone Diseases, Metabolic • Magnetic Resonance Imaging • X-Ray Film

PDF file: <http://www.polradiol.com/abstract/index/idArt/901601>

Background

The advent of advanced imaging in diagnostics has overshadowed plain radiography as the first-line imaging modality. The art of reporting plain radiographs and correlating them with MRI/computed tomography (CT) is gradually fading. Interpreting MR or CT images without glancing through plain radiographs often conceals important hints that might lead towards the diagnosis of particular pathological conditions. This, in turn, could lead to early treatment and good clinical outcomes. Accurate and reliable reporting of images is of crucial importance to clinicians for planning the mode and duration of treatment. Although advanced imaging can make important contributions in certain instances, plain radiography is widely regarded as the first-line imaging modality in bone and metabolic disorders [1]. This case-based pictorial review presents a comprehensive imaging spectrum of various bone pathologies that show non-specific findings on MRI.

Case-1

A 37-year-old lady presented to the rheumatology clinic with generalized body pain, inflammatory low backache and predominant lower limb arthralgia for two years. MRI of the lumbosacral spine and sacroiliac joint was done to rule out disc disease and spondyloarthritis. MRI revealed changes as shown in Figure 1A–1D. Concomitant plain radiographs of the lumbar spine and chest were evaluated (Figure 2A–2C) together with the MR images. Based on plain radiography findings, a presumptive diagnosis of primary hyperparathyroidism was considered. Further blood investigations and ultrasound of the neck confirmed the diagnosis of primary hyperparathyroidism caused by bilateral parathyroid adenoma (image not shown). Patient underwent surgery and was subsequently asymptomatic.

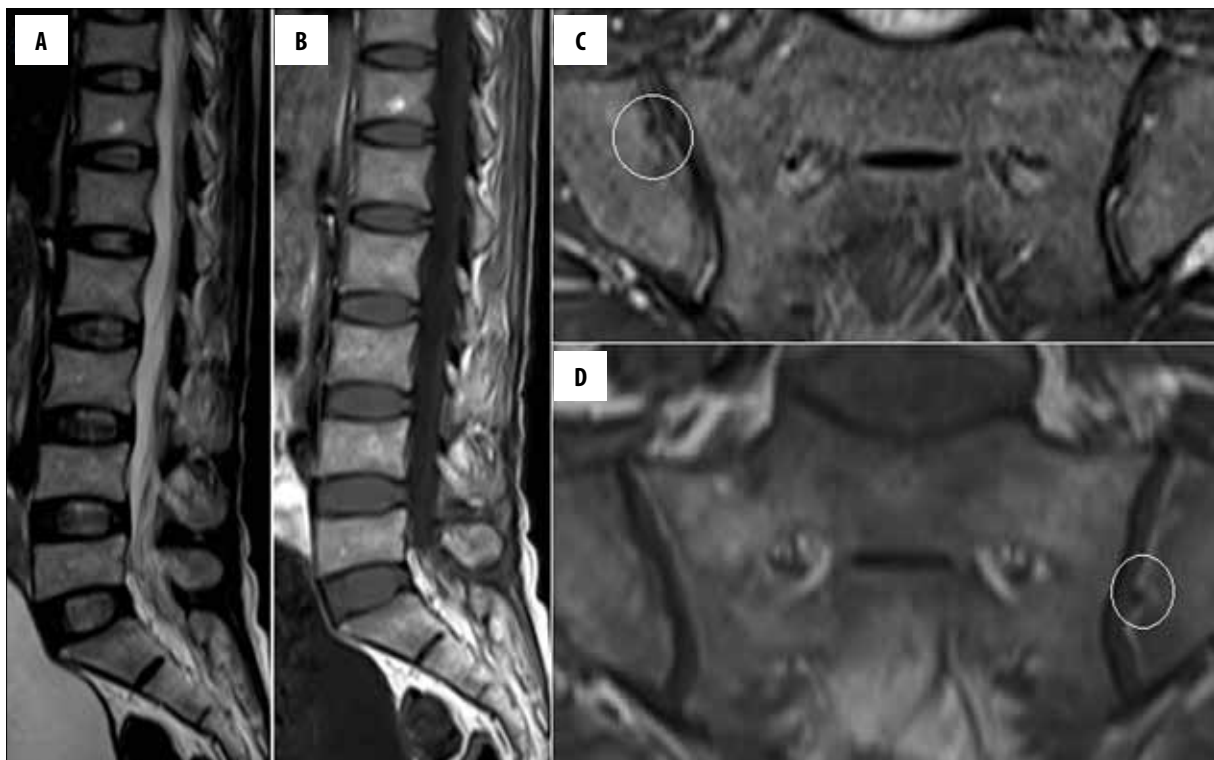


Figure 1. (A) T2-weighted (W) and (B) T1-W sagittal MR images of the lumbosacral spine showing a mild decrease in height of the visualized thoracolumbar vertebrae; (C) T2 fat-suppressed oblique coronal and (D) T1-W oblique coronal image of the sacroiliac joint showing mild irregularity along the iliac articular surface (circles), with no evidence of subchondral bone marrow oedema or significant erosion.

Case-2

A 27-year-old lady visited the rheumatology clinic with inflammatory back pain, generalized pain and inflammatory arthritis. As part of the evaluation, she underwent frontal radiographs of the pelvis, MRI of the lumbosacral spine and sacroiliac joint. MRI was inconclusive as shown in Figure 3A, 3B. However, the available plain radiographs demonstrated findings as described in Figure 4A, based on which a possibility of primary hyperparathyroidism was considered. Further lumbar spine and skull radiographs (Figure 4B, 4C) showed additional findings, as described. The patient underwent ultrasound of the neck and a Sestamibi parathyroid scan, which revealed a right-sided superior parathyroid adenoma (image not shown).

Case-3

A 52-year-old lady was evaluated for backache, difficulty in walking and weakness of both upper and lower limbs for two years. MRI of the lumbosacral spine and whole spine screening was done and showed non-specific minor degenerative changes (images not shown). The available plain radiographs reviewed at the time of MRI reporting demonstrated findings as shown in Figure 5A, 5B. Based on multiple pathological fractures on plain radiographs, severe hypophosphatemia and renal phosphate wasting seen in laboratory parameters, a diagnosis of oncogenic osteomalacia was considered. Further advanced imaging confirmed the presence of a pathological mass in the nasal cavity. Tumour excision and histopathological examination revealed a diagnosis of phosphaturic mesenchymal tumour.

Case-4

A 19-year-old girl consulted the rheumatology clinic with features suggestive of inflammatory backache. MRI of the lumbosacral spine and sacroiliac joint performed in order to rule out sacroiliitis was unremarkable (Figure 6A, 6B). The available plain radiographs revealed features of osteomalacia (Figure 7A, 7B). Abnormally low vitamin D concentration, mildly low serum calcium and phosphate levels in blood confirmed the diagnosis. The patient was started on vitamin D supplementation. She had a remarkable improvement at subsequent clinical follow up.

Case-5

A 61-year-old gentleman presented with a history of tightness of all four limbs for four years. MRI of the whole spine was performed. It showed non-specific degenerative changes, multilevel ligamentum flavum thickening and segmental posterior longitudinal ligament (PLL) thickening in the cervical spine, causing canal compromise and spinal cord compression with myelomalacic changes (images not shown). The available plain radiographs demonstrated findings as described in Figure 8A–8C. Based on plain radiographs, a diagnosis of fluorosis was suspected. Frontal radiograph of the forearm (Figure 8D) further confirmed the diagnosis.

Case-6

A 67-year-old gentleman presented to the orthopaedic outpatient clinic with multiple joint pain, right lower limb

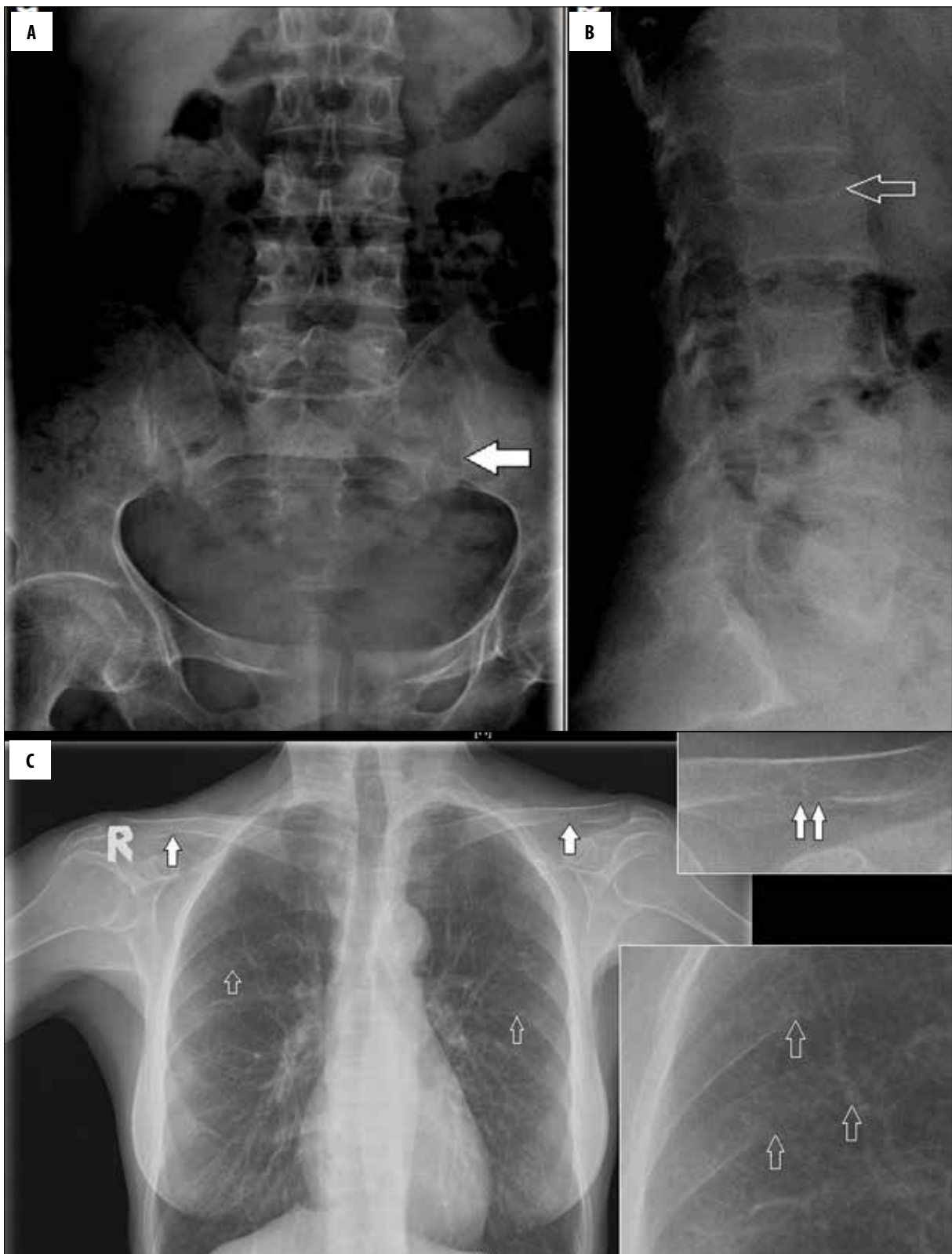


Figure 2. (A, B) Frontal and lateral radiographs of the lumbosacral spine showing diffuse osteopenia of all the visualized bones with fuzzy bone density, widening of the sacroiliac joint with irregularity of the cortical joint line suggesting subchondral resorption along the iliac side (solid arrow). Multilevel decrease in height of the vertebrae with biconcavity and thinning of cortices (open arrow) suggesting bone softening; (C) Chest radiograph shows an indistinct margin with subperiosteal resorption along the inferior aspect of posterior ribs in the midclavicular line (open arrows), more appreciated in a magnified view. Similar subtle subligamentous resorption along the inferior surface of distal clavicle, more on the left side, clearly seen in a magnified view.

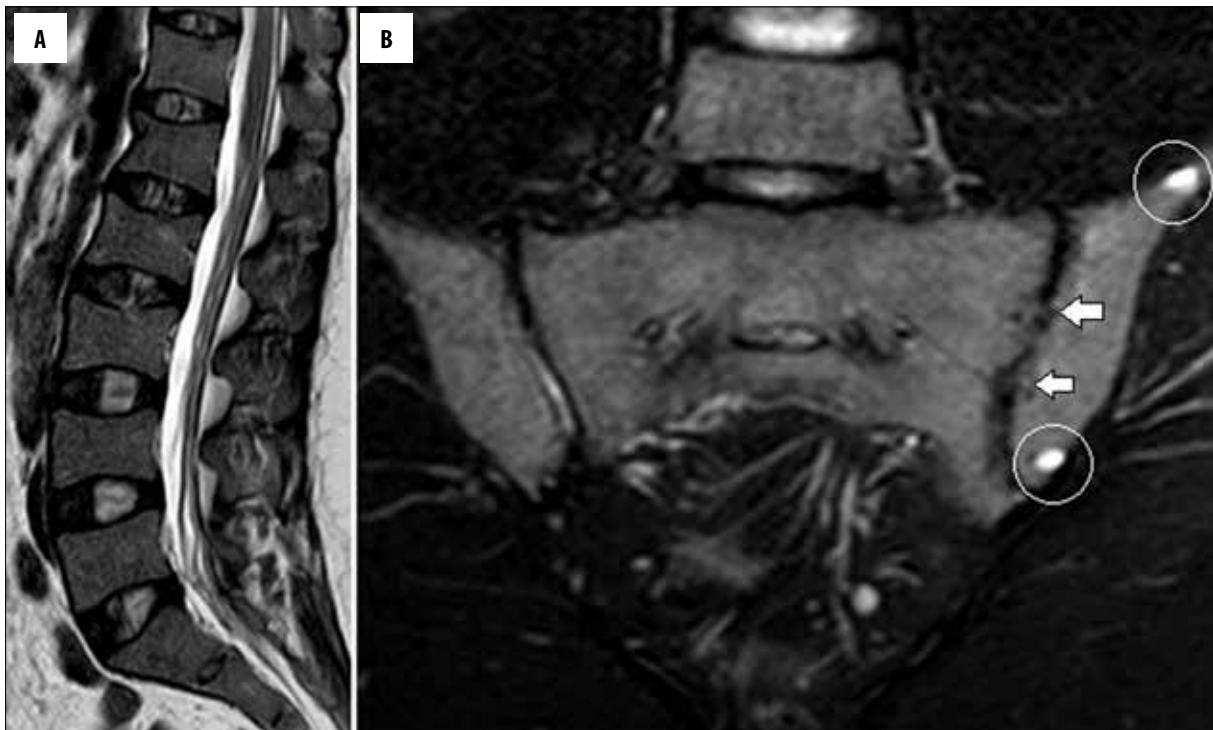


Figure 3. (A) T2-W sagittal MR image of the lumbosacral spine shows a mild decrease in height of the visualized thoracolumbar vertebrae; (B) T2 fat-suppressed oblique coronal view of the sacroiliac joint shows two small cysts (circles) in the left iliac bone with irregularity in the left iliac articular surface (arrows); however, no definite evidence of subchondral bone marrow oedema or large erosion is seen.

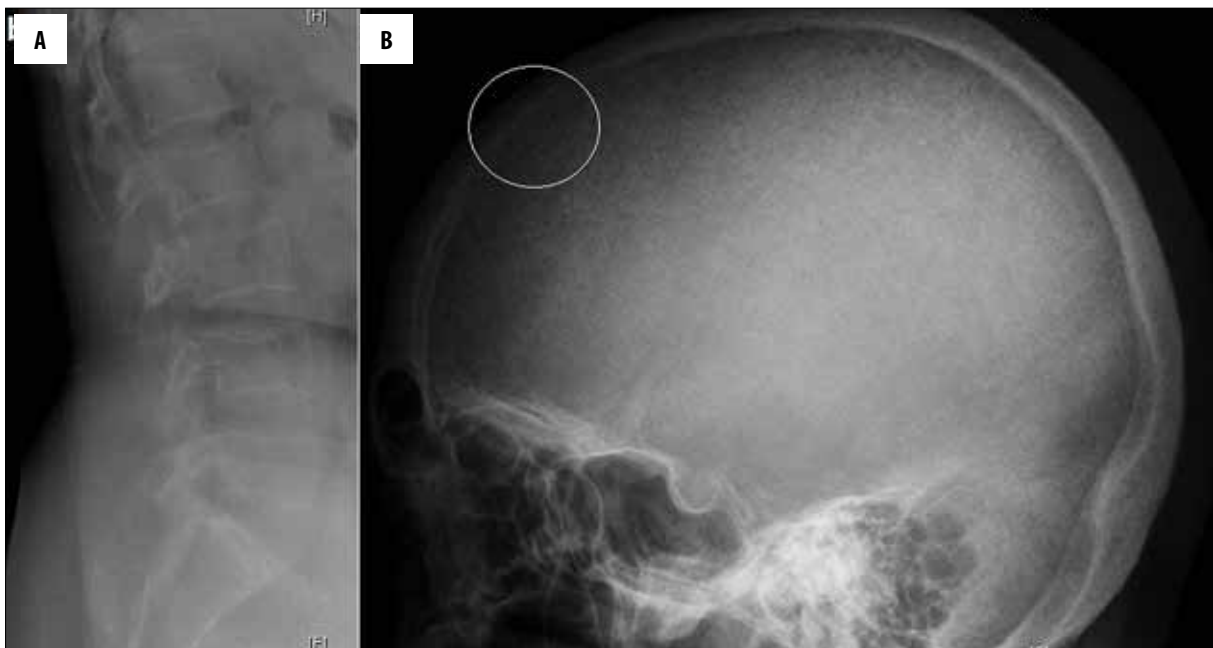


Figure 4. (A) Frontal radiograph of the pelvis shows mild diffuse osteopenia, subtle subperiosteal resorption along the medial cortex of the upper femur bilaterally (solid white arrows), more clearly seen in the zoomed image, in the form of subtle periosteal cortical irregularity (open arrows) as compared to the adjacent normal periosteal cortex (circle); mild irregularity along the iliac side (brown arrow) of the sacroiliac joint suggests subchondral resorption; subchondral resorption along the pubic symphysis with a mild widening (black arrow) and multiple lytic lesions (thin long arrows) suggest brown tumour in the left femur and iliac bones; (B) Lateral radiograph of the lumbar spine and (C) skull show a decrease in height of the vertebrae with biconcavity and thinning of cortices; loss of definition of the inner table of skull (circle) with multiple tiny hyperlucent areas in the skull vault caused by resorption of the tubercular bone, giving a "pepper pot" appearance to the calvarium.

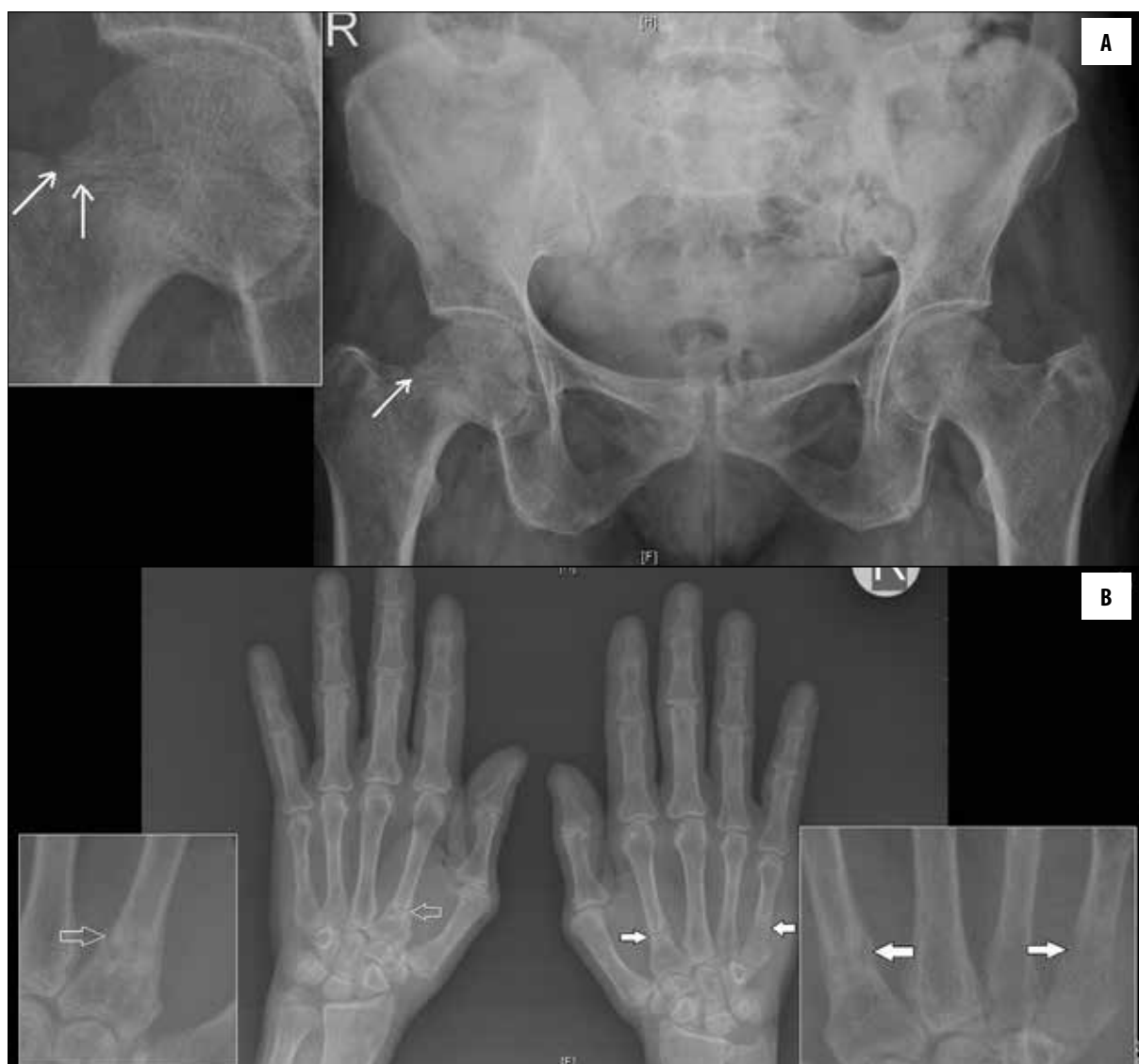


Figure 5. (A) Frontal radiograph of the pelvis shows mild diffuse osteopenia, a subtle incomplete fracture along the superolateral cortex of the neck of right femur, more clearly seen on the magnified view (arrows); (B) frontal radiograph of both hands shows diffuse osteopenia and multiple subtle irregular pathological fractures involving the base of metacarpals (arrows), more appreciated on magnified views.

weakness and right hip pain radiating to the knee. The pain increased on walking. MRI of the whole spine showed diffuse multilevel degenerative changes (images not shown). Plain radiographs were (Figure 9A–9C) suggestive of alkaptonuria.

Case-7

A 57-year-old gentleman was referred from a secondary care centre to the rheumatology clinic for further management of spondyloarthritis. His HLA-B27 allele was positive and CT of the SI joint was interpreted initially as bilateral chronic sacroiliitis. All the available radiographs (Figure 10A–10C) and CT (Figure 10D) were reviewed by a musculoskeletal radiologist, and a final diagnosis of diffuse idiopathic skeletal hyperostosis (DISH) was considered.

Case-8

A 28-year-old gentleman presented to the orthopaedic outpatient clinic with complaints of lower and mid-level back pain. MRI of the thoracolumbar spine was done to look for the underlying cause, which showed non-specific mild degenerative changes (Figure 11). Plain radiographs (Figure 12A–12C) were also reviewed, which suggested Scheuermann's disease.

Case-9

A 32-year-old gentleman presented to the clinic with a one-year history of low backache, generalized weakness and recurrent renal stone disease. MRI of the whole spine was performed to evaluate the back pain. It showed non-specific mild degenerative disease and a mild decrease in the bone marrow signal intensity (image not shown). The available plain radiographs were reviewed, which demonstrated

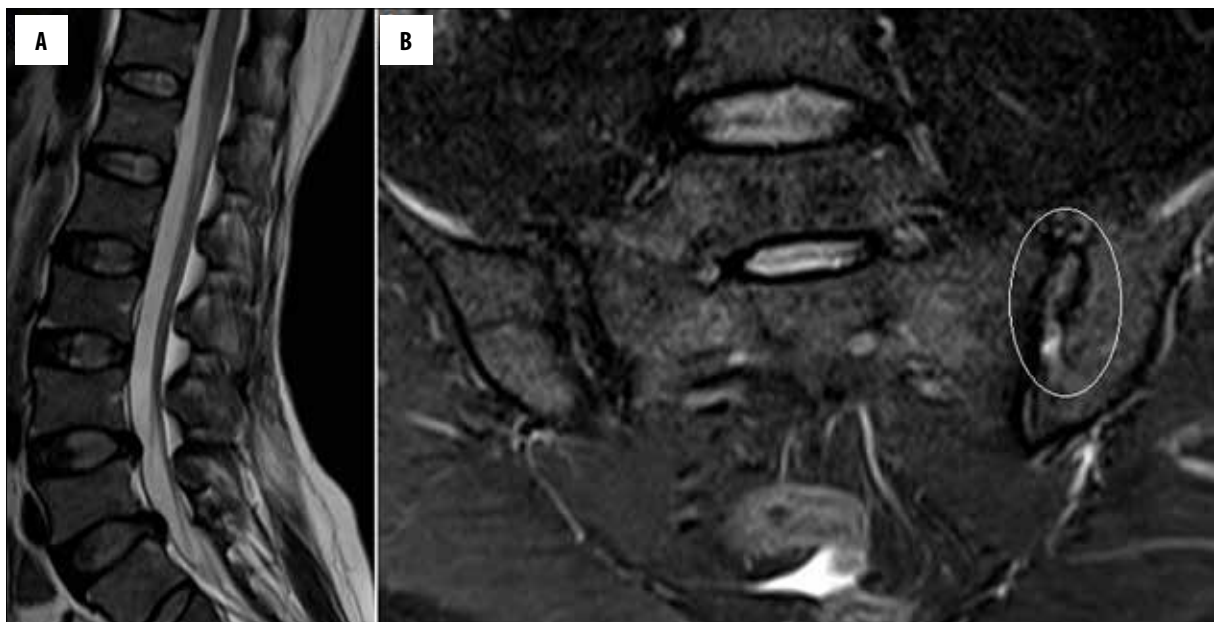


Figure 6. (A) T2-W sagittal MR image of the lumbosacral spine shows a mild decrease in height of the visualized thoracolumbar vertebrae with mild disc disease in the lower lumbar spine; (B), T2 fat-suppressed oblique coronal view of the sacroiliac joint shows mild irregularity along the iliac articular surface with widening of joint space (circle).

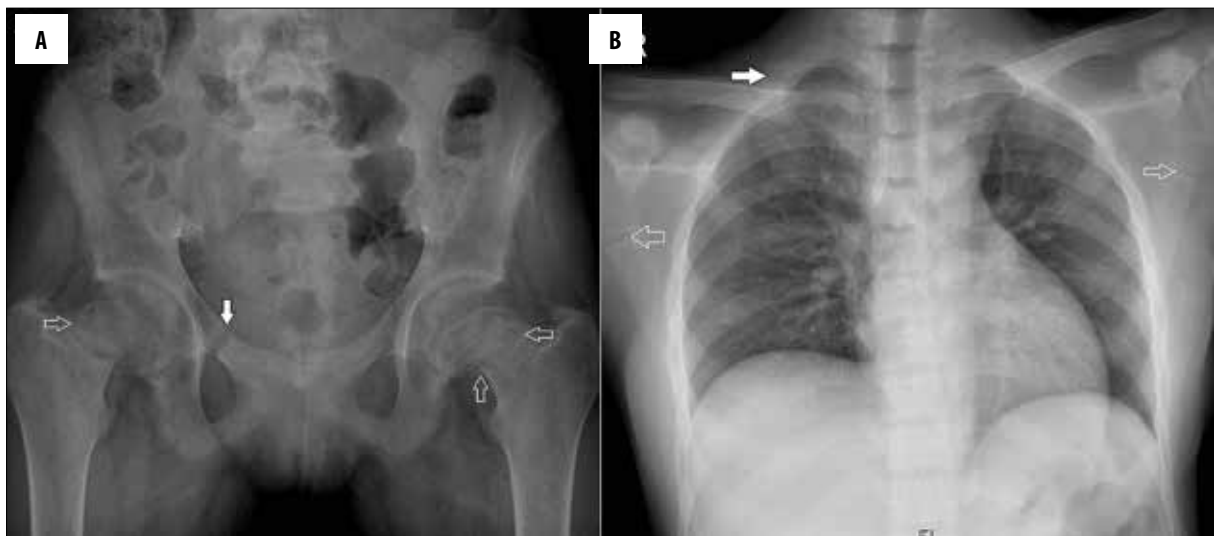


Figure 7. (A) Frontal radiograph of the pelvis shows mild diffuse osteopenia with fuzzy bone density and multiple lucent lines suggesting pseudo-fractures along the neck of both femur (open arrows) and right superior pubic ramus (solid arrow); (B) Frontal chest radiograph shows diffuse osteopenia and pseudo-fractures at the lateral border of scapula bilaterally (open arrows) and in the right first rib (solid arrow).

findings as shown in Figure 13A, 13B. Plain radiographs and deranged renal parameters aided in the diagnosis of renal osteodystrophy.

Case-10

A 24-year-old male presented to the orthopaedic clinic with pain in the sacrococcygeal region. Suspecting a clinical diagnosis of coccydynia, MRI of the lumbosacral and sacrococcygeal region was ordered. It (Figure 14A, 14B) confirmed the diagnosis of coccydynia and the orthopaedic surgeon planned corticosteroid injection into the sacrococcygeal joint. Plain radiographs of the lumbosacral spine (Figure 14C) suggested a diagnosis of bilateral symmetric

chronic sacroiliitis, which was further confirmed on a limited sacroiliac joint MRI scan (Figure 14D).

Discussion

Bone disorders of metabolic and endocrine origin are commonly encountered. They are characterized by abnormalities in calcium metabolism and/or intrinsic alterations in bone cell physiology [2,3]. Metabolic bone diseases comprise a heterogeneous group of acquired and inherited disorders, often difficult to distinguish based on the history and clinical examination [4,5]. They can have diverse radiological findings that are often diagnostic, albeit subtle [1]. Osteoporosis is the commonest type of metabolic bone



Figure 8. (A) Frontal radiograph of the pelvis shows diffusely increased bone density, trabecular thickening, thickening and ossification of the sacrotuberous ligament (solid arrow), ossification of the rectus femoris tendon attachment at the anterior inferior iliac spine (open arrow); (B, C) Lateral radiographs of the cervical and lumbar spine show a diffuse increase in bone density, thickening and ossification of the anterior (open arrow) and posterior (black arrow) longitudinal ligaments; (D) frontal radiograph of the right forearm shows interosseous membrane ossification (arrow).

classification criteria for spondyloarthritis, many of these patients undergo MRI of the sacroiliac joints and spine [8].

Radiological evaluation of these conditions can demonstrate typical appearances of the bones – decreased bone matrix, increased bone matrix or abnormal bone mineralization, depending on the underlying defect [5,7]. Predominant radiographic patterns of these conditions are decreased or increased bone density (osteopenia and osteosclerosis, respectively), and softening of bones leading to bowing, complete or incomplete fractures, as seen in rickets and osteomalacia [7]. Table 1 gives a comprehensive list of diagnostic radiographic signs of the various cases included in this series, which are commonly overlooked. Osteopenia can be seen in the spectrum of conditions such as osteoporosis, rickets, osteomalacia, scurvy, steroid therapy and endocrine disorders including acromegaly and hyperparathyroidism, while osteosclerosis can be seen in renal osteodystrophy, fluorosis, lead poisoning and hypervitaminosis A and D.

In osteoporosis, there is no defect in mineralization and osteoid formation [9]. However, a decrease in bone mass leads to radiographic abnormalities such as increased radiolucency, thinned cortices, altered trabecular patterns, insufficiency fracture and compression deformities of vertebrae including vertebra plana, wedged vertebrae, biconcave vertebrae and isolated end-plate deformities [7,9]. In rickets and osteomalacia, there is a defect in mineralization of normal osteoid tissue. Both these conditions usually result from an abnormality in vitamin D metabolism, but it could be due to renal tubular acidosis or vitamin D

disease, especially in the developed countries [6,7]. Other relatively common pathological processes that affect the skeleton are rickets, osteomalacia, scurvy, primary and secondary hyperparathyroidism and Paget's disease [1,7]. Patients with these conditions often present to orthopaedic surgeons or rheumatologists with non-specific back pain, polyarthralgia and generalised body pain, which mimic degenerative diseases of the spine or spondyloarthritis. Presenting symptoms often delude the clinicians in the diagnostic approach. With the inclusion of MRI in the ASAS

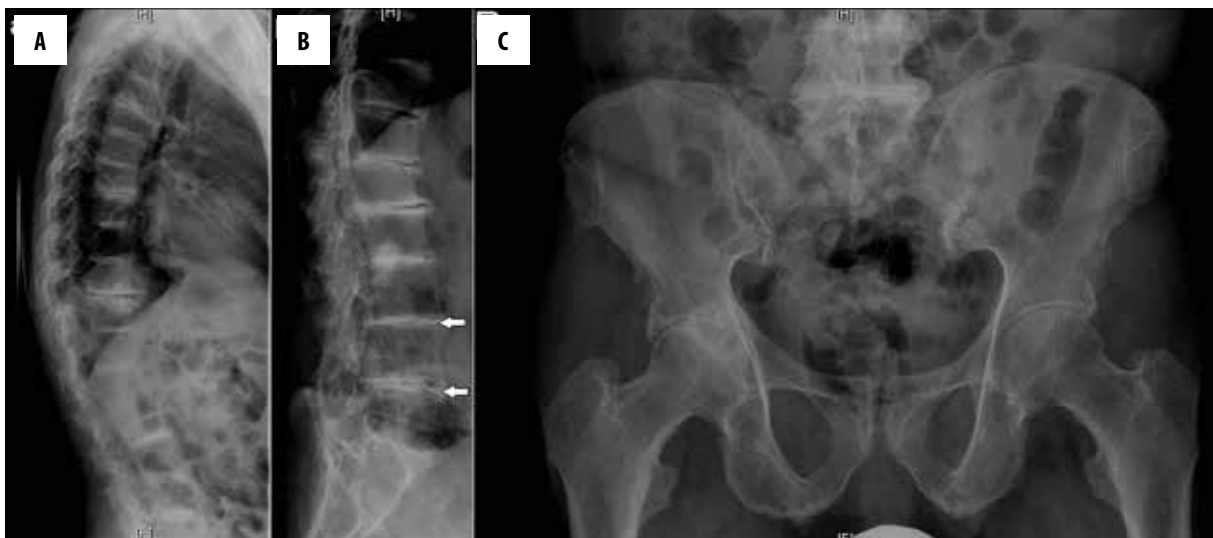


Figure 9. (A, B) Lateral radiographs of the thoracic and lumbar spine demonstrate multilevel disc space narrowing, intervertebral disc calcification (arrows), vertebral osteophytes and mild osteopenia; (C) Frontal radiograph of the pelvis shows degenerative arthritis of the right hip joint and both sacroiliac joints.

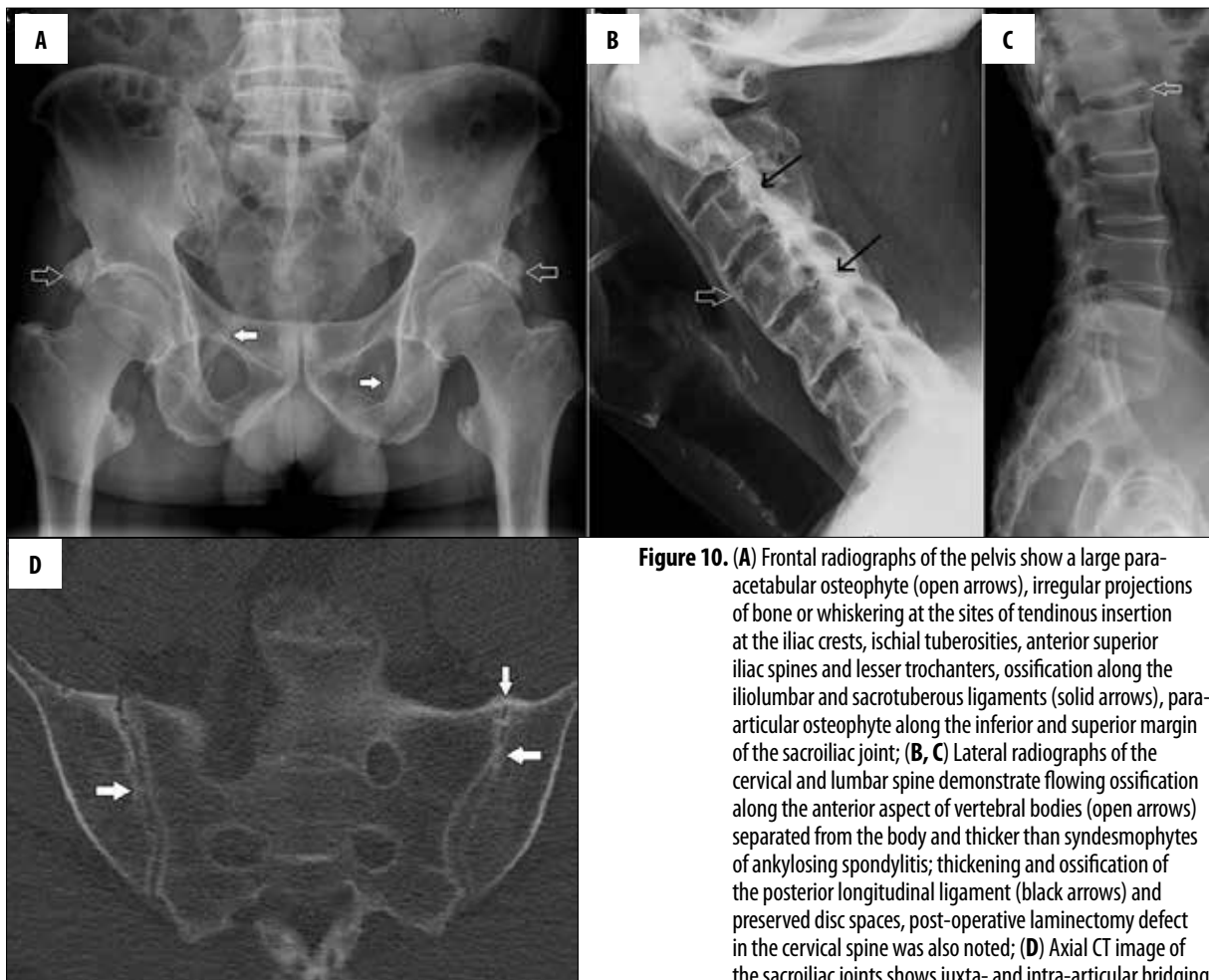


Figure 10. (A) Frontal radiographs of the pelvis show a large para-acetabular osteophyte (open arrows), irregular projections of bone or whiskering at the sites of tendinous insertion at the iliac crests, ischial tuberosities, anterior superior iliac spines and lesser trochanters, ossification along the iliolumbar and sacrotuberous ligaments (solid arrows), para-articular osteophyte along the inferior and superior margin of the sacroiliac joint; (B, C) Lateral radiographs of the cervical and lumbar spine demonstrate flowing ossification along the anterior aspect of vertebral bodies (open arrows) separated from the body and thicker than syndesmophytes of ankylosing spondylitis; thickening and ossification of the posterior longitudinal ligament (black arrows) and preserved disc spaces, post-operative laminectomy defect in the cervical spine was also noted; (D) Axial CT image of the sacroiliac joints shows juxta- and intra-articular bridging ossification with absence of articular surface erosion. The absence of erosions and joint space narrowing of the sacroiliac joint as well as facet joint ankylosis differentiate this disease from ankylosing spondylitis, and normal bone density differentiates it from fluorosis.



Figure 11. T2-W sagittal MR image of the lumbosacral spine shows a decrease in height of the vertebral bodies at the thoracolumbar junction with end-plate irregularity and minor degenerative changes

resistant rickets [7]. Primary and secondary hyperparathyroidism present with non-specific complaints of back pain and may show osteopenia or osteosclerosis, as depicted on radiographs [10,11]. Radiographs can show specific findings (as shown in Table 1) that are consistent with these disorders. Radiographs of the hands are sensitive in finding subperiosteal resorption [10,11]. Sacroiliac joint involvement by subchondral bone resorption resembles inflammatory sacroiliitis of spondyloarthropathy, and periarticular bone resorption may resemble rheumatoid arthritis. Focal deposition of amyloid and brown tumours may resemble neoplasm such as multiple myeloma. Further diagnosis of primary or secondary hyperparathyroidism is made by means of laboratory confirmation of an elevated PTH level, abnormal renal parameters and ultrasonography to exclude a parathyroid adenoma [12].

Another important entity that can clinically mimic spondyloarthropathy is DISH, as it can very well present with early morning stiffness. This can be extremely difficult to differentiate from spondyloarthritis, especially in middle-aged patients. An in-depth knowledge of radiographic findings (as shown in Table 1) is a prerequisite for diagnosing DISH, and if required, further characterization may be provided by cross-sectional imaging, including CT and

Figure 12. (A, B) Frontal and lateral radiographs of the thoracolumbar spine showing kyphosis of the spine at the thoracolumbar junction, anterior wedging of Th1 to L1 vertebrae, vertebral end-plate irregularity and intervertebral disc space narrowing, more clearly seen on (C) the magnified view (circle).

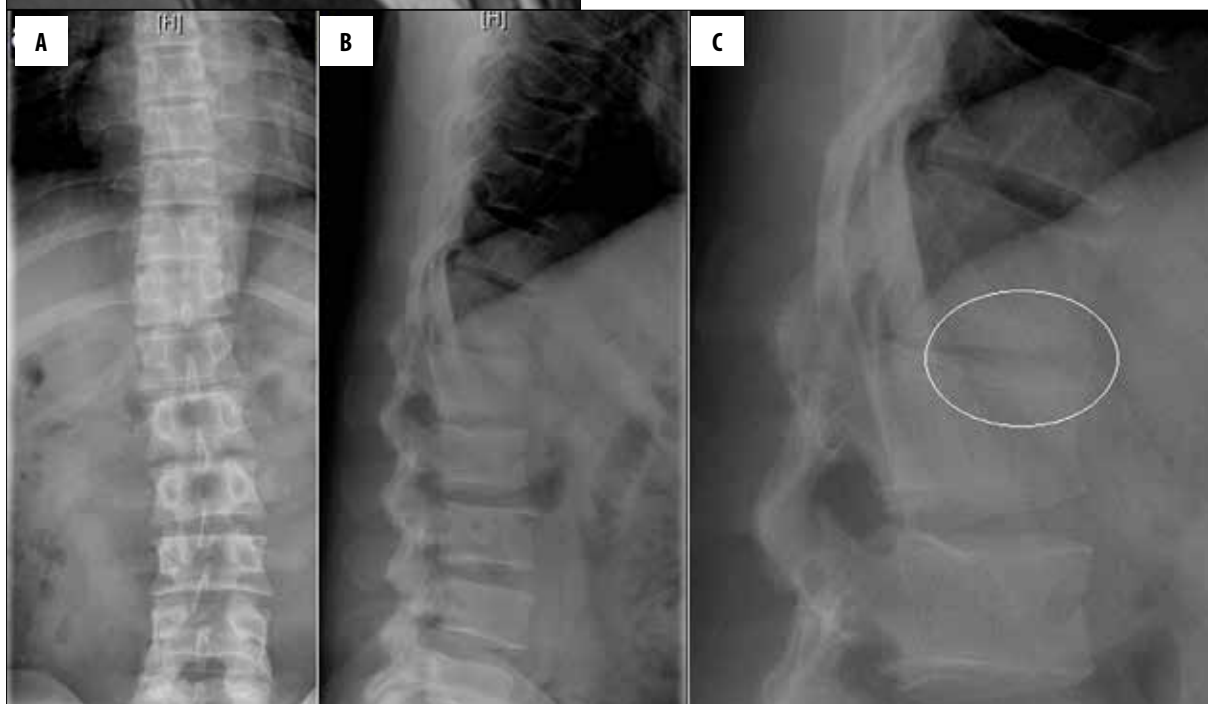
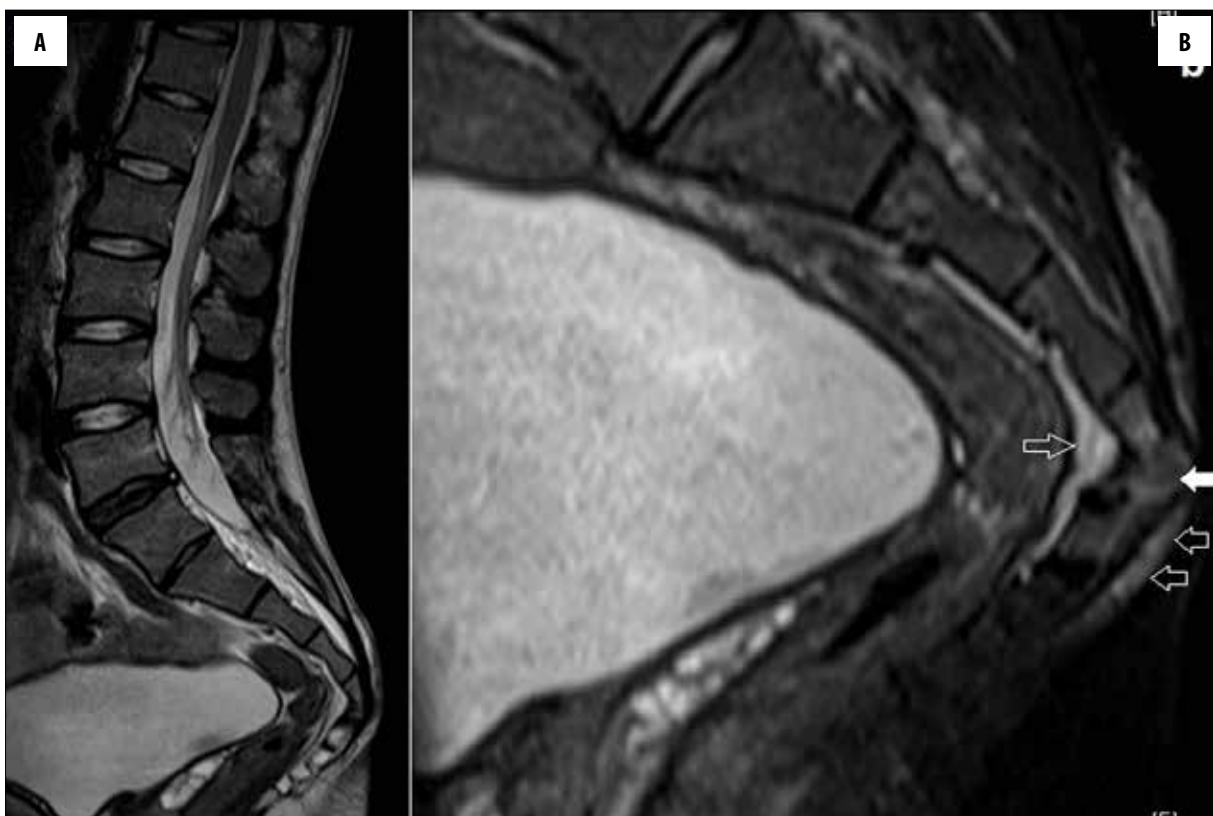




Figure 13. (A) Frontal radiograph of the pelvis shows diffusely increased bone density, pseudo-fractures at the superior pubic rami (solid arrows); mild widening of the sacroiliac joint space and irregularity along the iliac articular surface (open arrow) suggest osteomalacia, note the bilateral ureteric calculi; (B) lateral radiographs of the lumbar spine show dense end-plates giving appearance of a rugger-jersey spine (open arrow). Renal osteodystrophy combines features of secondary hyperparathyroidism, osteomalacia and osteoporosis.



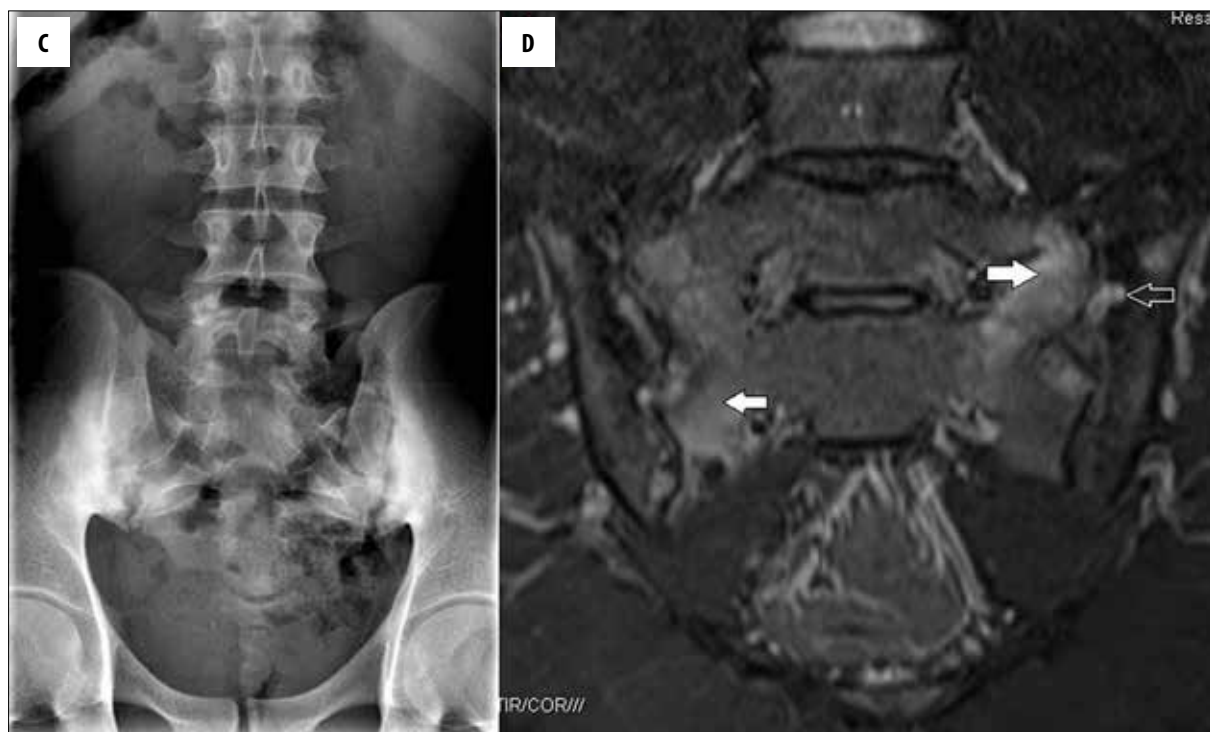


Figure 14. (A) T2-weighted sagittal view of the lumbosacral spine and (B) T2 fat-suppressed sagittal image of the sacroccygeal region show fluid at the sacroccygeal junction (solid arrow), adjacent bone marrow oedema and fluid anteriorly and posteriorly to the sacroccygeal segments in the bursa (open arrows); (C) Frontal radiograph of the lumbosacral spine shows bilateral near-symmetric chronic sacroiliitis in the form of subchondral sclerosis, multiple articular surface erosions and mild joint space narrowing; (D) later T2 fat-suppressed oblique coronal view of the sacroiliac joint shows bilateral subchondral bone marrow oedema (solid arrows), erosion (open arrows) and subchondral sclerosis.

Table 1. Subtle radiographic signs which should not be overlooked.

Diagnosis	Specific radiographic clues
Primary hyperparathyroidism	Diffuse osteopenia Subperiosteal resorption - fraying and lace-like appearance of outer cortex of bone Subchondral resorption (can be confused with erosions in an inflammatory arthritis) Trabecular resorption – “salt and pepper” calvarium Subligamentous and subtendinous changes Brown tumours Chondrocalcinosis
Osteomalacia	Fuzzy or dirty appearance of bone density Pseudo-fractures in pelvis, scapula and ribs Decreased vertebral body height Bowing of long bones
Rickets	Widened bulky physal plates Irregularity and splaying of bone at the junction of metaphysis and physis Slipped capital femoral epiphysis Bowing of long bones
X-linked hypophosphatemia or familial vitamin D-resistant rickets	Stress fracture with pronounced enthesopathic changes
Renal osteodystrophy	Diffuse osteosclerosis Biconcave vertebral bodies, with insufficiency fractures Rugger-jersey spine Soft tissue and vascular calcifications

Table 1 continued. Subtle radiographic signs which should not be overlooked.

Diagnosis	Specific radiographic clues
Fluorosis	Diffuse osteosclerosis (most common), can present with osteopenia Ossification of the attachments of tendons, ligaments and muscles Interosseous membrane ossification Ossification of the posterior longitudinal ligament Periosteal bone formation
DISH	No osteosclerosis Flowing ossification along the anterior or right anterolateral aspects of at least four contiguous vertebrae Usually well preserved disc spaces Interdigitating areas of protruding disc material in the flowing ossifications Absence of sacroiliac joint erosions, sclerosis or joint space narrowing however, juxta and or intraarticular bridging ossification can be present No apophyseal joint or costovertebral joint ankylosis Large osteophyte at the lateral margin of acetabulum
Alkaptonuria	Severe osteoporosis Multi-level intervertebral disc calcification Multi-level disc space narrowing Syndesmophyte formation Early marked osteoarthritic changes

MRI [13,14]. Chronic metabolic conditions such as skeletal fluorosis can also present with non-specific symptoms. They can have variable radiographic patterns (as shown in Table 1).

Conclusions

This pictorial review highlights the important radiographic features that can be missed if not looked for carefully. While MRI has certainly revolutionized the field of imaging, it is still not the panacea for the diagnosis of many

disorders. Plain radiographs still play a pivotal role in the armamentarium of radiology techniques. Investigations of the bone should start with plain radiography, which again should be interpreted carefully alongside clinical data, and if deemed necessary, other modalities can be relied upon for confirmation.

Conflicts of interest

No conflicts of interest or sources of financial support for this paper.

References:

- Cooper KL: Radiology of metabolic bone disease. *Endocrinol Metab Clin North Am*, 1989; 18: 955-76
- Rosen C (ed.): *Primer on the metabolic bone diseases and disorders of mineral metabolism*. American Society of Bone and Mineral Research; 7th edition, 2008
- Haugeberg G: Imaging of metabolic bone diseases. *Best Pract Res Clin Rheumatol*, 2008; 22(6): 1127-39
- Mankin HJ: Metabolic bone disease. *J Bone Joint Surg Am*, 1994; 76: 760
- Reynolds WA, Karo JJ: Radiologic diagnosis of metabolic bone disease. *Orthop Clin North Am*, 1972; 3: 521
- Adams JE: Advances in bone imaging for osteoporosis. *Nature Reviews Endocrinology*, 2013; 28-42
- Patel AA, Ramanathan R, Kuban J, Willis MC: Imaging findings and evaluation of metabolic bone disease. *Advances in Radiology*, 2015; 21
- Rudwaleit M, van der Heijde D, Landewe R et al: The development of assessment of spondyloarthritis international society classification criteria for axial spondyloarthritis (part II): validation and final selection. *Ann Rheum Dis*, 2009; 68: 777-83
- Guglielmi G, Muscarella S, Bazzocchi A: Integrated imaging approach to osteoporosis: state-of-the-art review and update. *Radiographics*, 2011; 31: 1343-64
- Murphey MD, Sartoris DJ, Quale JL et al: Musculoskeletal manifestations of chronic renal insufficiency. *Radiographics*, 1993; 13: 357-79
- Pugh DG: Subperiosteal resorption of bone; A roentgenologic manifestation of primary hyperparathyroidism and renal osteodystrophy. *Am J Roentgenol Radium Ther Nucl Med*, 1951; 66: 577-86
- Gritzmann N, Koischwitz D, Rettenbacher T: Sonography of the thyroid and parathyroid glands. *Radiol Clin North Am*, 2000; 38: 1131-45
- Resnick D: Diffuse idiopathic skeletal hyperostosis. In: Resnick D (ed.), *Diagnosis of bone and joint disorders*. 4th ed. Philadelphia, PA: Saunders, 2002; 1476-503
- Dar G, Peleg S, Masharawi Y et al: The association of sacroiliac joint bridging with other enthesopathies in the human body. *Spine*, 2007; 32: 303-8